

**UNIVERSITY OF BUCHAREST
FACULTY OF CHEMISTRY
DOCTORAL SCHOOL IN CHEMISTRY**

DOCTORAL THESIS

-summary-

PhD student:

Florin Bîlea

PhD Supervisor:

Prof. Dr. Andrei Valentin Medvedovici

2025

**UNIVERSITY OF BUCHAREST
FACULTY OF CHEMISTRY
DOCTORAL SCHOOL IN CHEMISTRY**

DOCTORAL THESIS

**Plasma degradation mechanisms of organic contaminants mixtures
in water
-summary-**

PhD student:

Florin Bîlea

PhD Supervisor:

Prof. Dr. Andrei Valentin Medvedovici

2025

Pollution has been recognized as one of the main challenges of the modern world, being associated with the continuous technical and technological development of society through industry, agriculture and medicine [1–3]. Water pollution was first regulated at European level in 1983 [4], legislation followed in 2000 by a directive establishing the legal framework in the field of water [2]. The latter has undergone various additions aimed at updating water quality standards [5] and compounds of interest that require monitoring, mainly including pharmaceuticals, pesticides and industrial by-products [6–10].

The medical field is one of the major sources of organic pollutants in water, in the form of active substances in drugs used to treat various medical conditions. The presence of pharmaceutical compounds in urban wastewater and groundwater originates both from hospital consumption and domestic use [11–13]. In general, their concentrations in hospital wastewater ranges from a few tens or hundreds of ng/L to hundreds of µg/L, and even mg/L in some cases. These concentrations can vary significantly in time and in space. Among the most common pollutants, analgesics, anti-inflammatories, and antibiotics are enumerated [14–17]. Generally, conventional treatment is ineffective for removing pharmaceutical contaminants from wastewater, resulting in their presence in natural waters [14, 15, 18–20].

The persistence of pharmaceutical pollutants following the application of conventional treatment methods has emphasized the need to develop new treatment methods that enable contaminants elimination and ensure adequate standards of treated water established at European Union level by “Directive (EU) 2024/3019 of the European Parliament and of the Council of 27 November 2024 concerning urban wastewater treatment” [21]. Advanced oxidation processes (AOPs) are such advanced treatment methods that have been intensively investigated during the last decades. They generally involve the use of very powerful oxidants, namely the hydroxyl radicals, for the degradation of organic pollutants of various origin. AOPs can be classified according to the method used to generate hydroxyl radicals, such as: ozonation at alkaline pH and catalytic ozonation, Fenton and photo-Fenton processes, UV-based processes such as photocatalysis, the peroxone process (the reaction between ozone and hydrogen peroxide), and, last but not least, the non-thermal plasma [22] investigated in this paper.

Depending on the AOP used, other reactive species besides hydroxyl radicals can contribute to the degradation of pollutants. Thus, non-thermal plasma generated at atmospheric

pressure in contact with water produces hydroxyl radicals from water molecules, as well as other reactive oxygen species (ROS) (HO^\bullet , O , O_3 , H_2O_2 etc.) and reactive nitrogen species (RNS). The main advantage of non-thermal plasma over other AOPs consists in the ability to produce these oxidative species in situ, using only electrical energy [23, 24]. Various reactor geometries have been experimentally investigated, the configurations that provide a large contact surface area between the plasma and the treated solution demonstrating the highest efficiency.

Thus far, the literature dealing with the degradation of pollutants from complex solutions has yielded varied results. Sometimes the pollutant removal is delayed when compared with individual solutions, while other times the elimination is accelerated. Due to these apparently contradictory results, it is difficult to modulate the discharge operation parameters to address the effect of the impurity matrix. Such adjustments would require either increasing the intensity of treatment, for situations when the degradation is slowed down, or limiting treatment in order to cut down costs when the impurity matrix has a positive effect. Therefore, there is a need for a better understanding of the processes that take place during plasma degradation of pollutants in mixtures. The studies published thus far have one common weakness: it is difficult to compare the results (degradation, yield, efficiency, etc.) obtained for mono-component solutions with those of complex mixtures of pollutants, characterised by different organic load. Another overlooked aspect concerns the degradation mechanisms, as the literature rarely differentiates between the contribution of various reactive species towards the pollutant removal in solution with complex impurity matrices. The interaction of degradation products with each other and with the target pollutants has rarely been investigated, either in mono- or in multi-component solutions.

Thus, the purpose of this work was to identify the mechanisms involved in the plasma degradation of organic pollutants in mono- and multi-component solutions, as well as to evaluate the impact of the impurity matrix. Specifically, the following objectives were pursued:

O1: Optimization of the discharge configuration and operating parameters to obtain fast and efficient degradation of organic contaminants with various chemical structures.

O2: Identification of degradation intermediates of the target pollutants in mono-component solutions.

O3: Identification of possible mechanisms responsible for the formation of the detected intermediates, starting from the reactive species present during treatment.

O4: Evaluation of the target pollutants degradation in solutions with complex impurity matrices.

O5: Evaluation of the degradation intermediates variation in terms of abundance and structure, as well as assessment of changes in the reaction mechanisms that occur when altering the impurity matrix.

In this work, a pulsed corona discharge above water and a dielectric barrier discharge were used, both operated with the recirculation of the contaminant solution. The corona discharge was operated in two experimental configurations: with and without recycling the surplus ozone generated in the discharge. Recycling ozone by bubbling it through the pollutant solution promotes its solubilization by increasing the contact surface area, potentially leading to improved degradation.

The first experimental part of this thesis (**Chapter 3**) focused on the optimisation of the experimental setup and operating parameters of the corona discharge using amoxicillin (AMX) (**O1**) as target pollutant. The other objectives of this study were to identify the degradation products (**O2**) and the mechanisms involved in their formation (**O3**).

During the optimization the following criteria were considered: the highest and fastest elimination and mineralization of the selected pollutant and high energy yield, associated with enhanced efficiency and, implicitly, reduced costs. The optimization of the operating parameters involved the evaluation of pollutant removal as a function of the electrical parameters, the discharge gas and the solution properties. With respect to the electrical parameters, experiments were performed by varying the duration of the high-voltage pulses (FWHM – "Full Width at Half Maximum") and the pulse frequency, resulting in changes of the power dissipated in the discharge. In order to evaluate the impact of pulse width, high voltage pulses of 106 ns and 300 ns were investigated. The longer pulses resulted in superior degradation of the contaminant, but the substantial difference between the average discharge power values (5.2 W vs. 27 W) must be taken into account. In order to achieve an average power of 27 W while using 106 ns pulses, the frequency was increased from 25 Hz to 115 Hz. For the same discharge power, the shorter pulses lead to faster degradation of the pollutant than the longer ones. The most effective degradation was recorded using short pulses at low frequency. The higher energy yield obtained in this case

is accompanied by slower degradation. Thus, pulses with FWHM of 106 ns at a frequency of 25 Hz were selected as optimal and were used in subsequent experiments.

Regarding the experimental setup optimization, the degradation of AMX with and without bubbling the effluent gas from the plasma through the liquid was compared. The ozone present in the effluent gas can react directly with the contaminant in solution contributing to its degradation, or it can decompose through reactions with various species, generating other ROS, which in turn can be involved in the degradation process. Perhaps the most notable ozone decomposition reaction that takes place in the plasma-ozonation system is the perozone process, which is the reaction between ozone and hydrogen peroxide formed from the combination of hydroxyl radicals. The perozone process produces hydroxyl radicals which can contribute to pollutant removal to a larger extent than the two active species that serve as its precursors. The plasma-ozonation setup thus created leads to an increase in efficiency of 6-7 times compared to plasma treatment, from 5-6 g/kWh to 35,5 g/kWh for the same removal (54%).

The influence of the gaseous atmosphere on the degradation of the pollutant was evaluated by comparing the results obtained with oxygen and air as discharge gases. The experimental setup was operated using both available configurations: plasma and plasma-ozonation. In the case of plasma treatment, the degradation of AMX does not depend significantly on the nature of the discharge gas. However, this becomes important in the plasma-ozonation configuration, where oxygen leads to much faster elimination of the antibiotic. The considerably slower degradation of AMX using air as discharge gas as compared to oxygen can be attributed to the generation of fewer ROS as a result of the lower partial pressure of oxygen. The RNS formed in air discharge are less reactive towards the organic compounds investigated, and in addition, they can react with ROS, further decreasing the amount available for the degradation of the target pollutant [25, 26].

In order to evaluate the effect of solution properties on the degradation, the conductivity, pH and the salts present in the solution were varied. Thus, the removal of AMX was investigated in the conductivity range 200-500 $\mu\text{S}/\text{cm}$. A slightly slower degradation of the antibiotic and a decrease in efficiency was observed for higher conductivity values.

The impact of pH on the removal efficiency of the target compound is often correlated with its molecular structure, as cationic and anionic forms of the molecules may have different reactivities towards the reactive oxygen and nitrogen species (RONS) generated in plasma. In

order to evaluate the pH influence, the degradation of AMX in solutions with initial pH of 3.7, 6.7 or 10 was investigated. Comparable results were obtained under acidic conditions and in solutions with initial pH of 6.7. The fastest elimination of the pollutant was obtained in the alkaline solution exposed to plasma. The initial pH values suffered changes as a result of the treatment: after 60 min, the final pH of the pH 3.7 and 6.7 solutions reached around 4, while the pH 10 solution reached 6.3.

In order to assess the influence of the salts, the solutions were prepared using sodium sulfate alone or together with sodium bicarbonate. In the presence of carbonate/bicarbonate anions, the solution is buffered during treatment, so the pH remained close to the initial value (in the range of 7.4-8.1), unlike the Na₂SO₄ solution, which quickly became acidic (pH 3.8-4.4) as a result of plasma exposure. Buffering the solution had a positive effect on the degradation as a result of maintaining alkaline pH. The pollutant removal occurred satisfactorily even in tap water, reaching an efficiency of 57 g/kWh at a removal of 93%, after only 5 minutes of treatment.

The degradation intermediates of AMX were identified based on the isotopic profile, exact mass and MS² spectra [27] recorded in positive ((+)ESI) and negative ((-)ESI) ionization modes. For the identification, the mass spectra of AMX and the associated fragmentation profiles played an important role. In (+)ESI, the compound sequentially loses the amino group as NH₃, the carbonyl group in the β-lactam cycle as CO, and the carboxyl group as CO₂. Loss of carboxyl and amino groups are also observed in (-)ESI. An important fragment for the identification of degradation intermediates was the (+)m/z 160 ion, associated with the thiazolidine cycle and its specific substituents. The presence of this fragment in the spectra of intermediate products shows the preservation of this moiety, which indicates that chemical changes occur in other parts of the molecule. Other fragments identified during the analysis that played an important role in products identification were (-)m/z 79.96 and (-)m/z 80.97, generally associated with SO₃^{•-} and HSO₃⁻ anions, fragments specific for sulfonated compounds.

In total, 26 potential degradation intermediates were identified and grouped into four major degradation pathways. The first degradation pathway involved the formation of AMX sulfoxide by oxidation of the sulphur atom in the structure of the thiazolidine cycle as a result of reaction with ozone or hydroxyl radicals. This pathway further describes the formation of the majority of sulfonated intermediates that serve as a source of reactive sulfur species (RSS). The

second pathway starts from the hydroxylation of the benzene ring of AMX through the addition of a hydroxyl radical to the double bond. The organic radical thus formed undergoes hydrogen abstraction after the attack of a second hydroxyl radical, which leads to the reformation of the double bond. Most notably, this intermediate serves as precursor for sulfonated intermediates as a result of the reaction with RSS obtained from the previously described degradation pathway. Sulfonation of the benzene ring takes place most likely through a mechanism similar to that of hydroxylation. The third degradation pathway involves opening of the β -lactam cycle with the formation of a penicilloic acid, which can be in turn degraded by hydroxylation, decarboxylation or cyclization. The latter involves the loss of a water molecule and the formation of diketopiperazine products. The fourth pathway starts with the oxidation and loss of the amino group. In addition to the hydroxylation mechanism, mechanisms were proposed for the acid hydrolysis of the β -lactam cycle with the formation of the corresponding penicilloic acid and the radical decarboxylation that leads to the elimination of a carboxyl group.

Most of the identified degradation intermediates are formed and subsequently degraded completely within the first 40 minutes of treatment in the plasma-ozonation system. Only seven products are still present in the solution treated for the longest time (60 min), of which only three still have cycles in their structure.

The second experimental part of this thesis (**Chapter 4**) used sulfamethoxazole (SMX) as target pollutant and aimed to evaluate its degradation using the previously optimised operating parameters (**O1**). Additionally, the degradation products (**O2**) and the chemical mechanisms involved (**O3**) were investigated. The corona discharge was used in plasma-ozonation configuration, operated in oxygen with pulses of 110 ns at a frequency of 25 Hz. The pollutant solution was prepared using tap water (pH 7.4-7.9, conductivity 260-280 $\mu\text{S}/\text{cm}$) and the initial concentrations of SMX were varied in the range 0.1-0.5 mM. The removal of the pollutant by non-thermal plasma treatment followed a pseudo-first order kinetic. The highest value of the apparent reaction rate constant ($k_{0.1} = 0.49 \text{ min}^{-1}$) was recorded for the lowest concentration of SMX (0.1 mM) in solution, and increasing the pollutant concentration caused a reduction in the reaction rate constant. The energy yield varied in the range 20-42 g/kWh (at 90% degradation), the process being more efficient for higher concentrations. These values exceed by more than one order of magnitude the already published data, which were around 1-1.5 g/kWh.

A total of 38 potential intermediates of degradation have been identified, of which only 12 have been previously reported in the literature. As in the case of AMX, the molecular formula was identified based on the isotopic profile and exact mass, while the proposed structures were based on the MS² spectra and the fragmentation profile of SMX. The main fragmentation pathway of this compound is described by the cleavage of the sulfonamide bond (**Figure 1.(A-B)**) resulting in the alternative formation of the (+)m/z 156 and (+)m/z 99 ions, with corresponding mass losses of 98 u and 155 u, respectively.

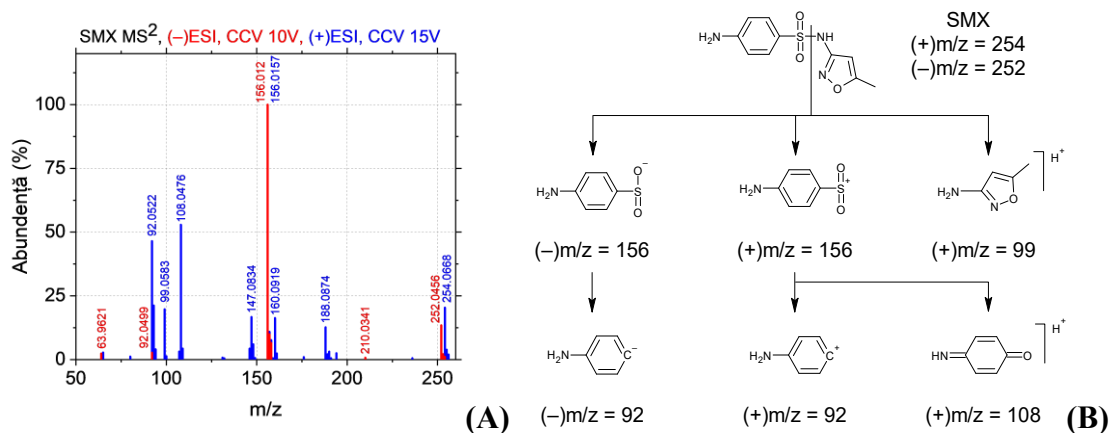


Figure 1. (A) MS² spectra of SMX recorded in (+/-)ESI; (B) The proposed fragmentation profile of SMX based on the recorded spectra. (CCV – collision cell voltage)

The subsequent fragmentation of the (+)m/z 156 ion leads to formation of (+)m/z 108 by the loss of SO ($\Delta m = 48$ u) or of (+)m/z 92 through the loss of SO₂ ($\Delta m = 64$ u). The direct removal of SO₂ from the precursor ion was also observed, leading to the formation of the (+)m/z 188 fragment. In (-)ESI, the precursor ion was represented by the deprotonated form of SMX, having (-)m/z = 252. Its fragmentation led to the formation of the (-)m/z 156 ion and a neutral loss of 96 u. Subsequent fragmentation leads to the formation of the ions (-)m/z 92 and SO₂⁻ ((-)m/z 64). These fragments served as a starting point in the interpretation of the mass spectra of SMX degradation intermediates. Their presence supports the conservation of the associated structure, while the absence indicates chemical changes of the same moiety. An example of such behaviour was observed for the mono-hydroxylated intermediates of SMX (S269abc). In the mass spectra of S269a, the ions (+/-)m/z 156, (+/-)m/z 92, (+)m/z 108 from the SMX spectra were observed, but not (+)m/z 99, the latter being replaced by (+)m/z 115. The mass difference of 16 u indicates an additional oxygen atom, consistent with the hydroxylation of 3-amino-5-

methylisoxazole. In the case of S269bc, the opposite situation occurred: the presence of (+)m/z 99 and the absence of the other fragments which were replaced by (+/-)m/z 172 ((+/-)m/z 156 + 16 u), (+)m/z 124 ((+)m/z 108 + 16 u) and (+/-)m/z 108 ((+/-)m/z 92 + 16 u), corresponding to the hydroxylation of the benzene ring.

Other fragments essential for identifying the structure of the degradation intermediates were: (+/-)m/z 161, (-)m/z 97, (-)m/z 81 and (-)m/z 80. Among these, (-)m/z 97 is the (-)ESI equivalent of the (+)m/z 99 ion in the (+)ESI spectrum of SMX, while (-)m/z 81 and (-)m/z 80 are associated with the $\text{SO}_3^{\bullet-}$ and HSO_3^- anions, similar to the case of AMX described above. The (+/-)m/z 161 fragment has been associated with the cleavage of the C–S bond in the structure of SMX, which is not represented in its mass spectra but is found in the spectra of some degradation products. Thus, this fragment shows the preservation of 3-amino-5-methylisoxazole.

The identified intermediates were grouped into five degradation paths, starting from different reactions of the reactive species with SMX. Two of the pathways involved hydroxylation of either the benzene or the isoxazole ring. Another pathway starts from the C–S bond cleavage, and a fourth describes the oxidation of the methyl group of the isoxazole ring to carboxyl. The last route involved the reaction of SMX with a $\text{SO}_4^{\bullet-}$ radical forming an organosulfate that subsequently degrades yielding the equivalent hydroxylated intermediate.

During the products further degradation, multiple reactions take place, including: hydroxylation, oxidation, sulfonation, decarboxylation, dimerization, fragmentation, cyclization and opening of cycles, including opening of the benzene ring. For some of these reactions, mechanisms based on the existing literature have been proposed. Thus, the previously described two-step radical hydroxylation mechanism leads to the formation of multiple hydroxylated degradation intermediates. This mechanism is also applicable for two-step sulfonation reactions with the participation of $\text{SO}_3^{\bullet-}$. The mechanism leading to the opening of the benzene ring is somewhat more complicated (**Figure 2.**). It involves the addition of an ozone molecule to a double bond of the benzene ring resulting in the formation of an unstable ozonide. This compound reacts with water, forming an organic peroxide and opening the cycle. The resulting intermediate loses H_2O_2 and becomes the recorded stable product.

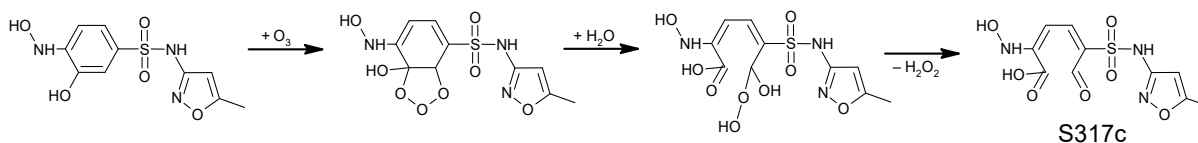


Figure 2. Reaction mechanism describing the benzene ring opening of N-hydroxylated intermediates of SMX through reaction with ozone

An unexpected reaction that occurred during SMX degradation was dimerization. This reaction mechanism is initiated by the pollutant fragmentation forming an aniline radical, which can react with a SMX molecule leading to a product containing an aniline dimer in its structure (**Figure 3**).

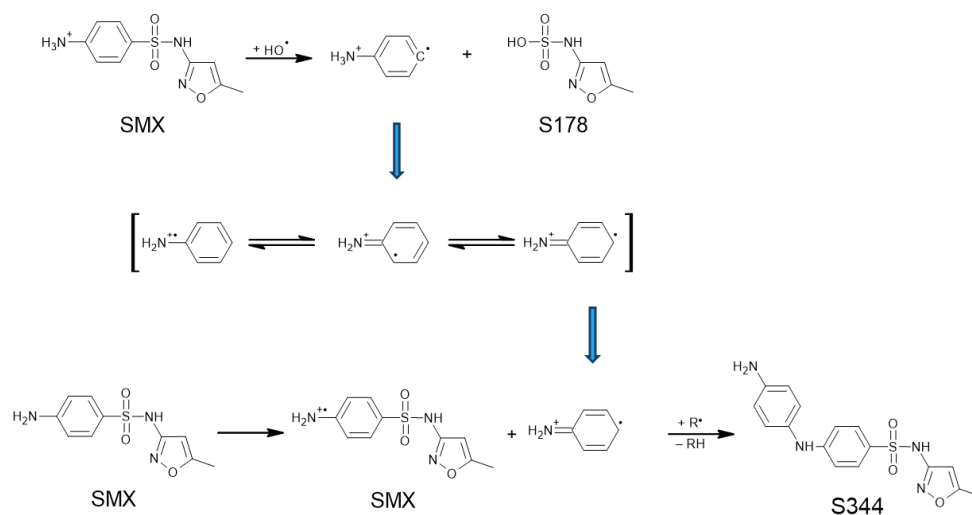


Figure 3. Aniline dimerization mechanism involved in the formation of S344 intermediate.

Another unexpected mechanism was that of benzene ring opening followed by cyclization (**Figure 4**). This is a mechanism specific to aromatic amines which starts, as previously described, with the addition of ozone to the double bond forming an ozonide that decomposes through the reaction with water. This time the elimination of the water molecule is done with the participation of the amine group, which leads to the formation of pyridine-2-carboxylic acid and water.

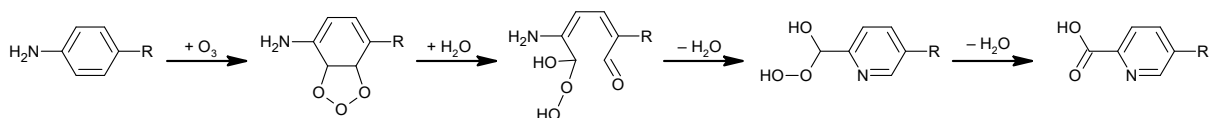


Figure 4. Opening of the benzene ring of the aniline moiety through reaction with ozone, resulting in cyclization and formation of a pyridine cycle.

It is important to note that some intermediates are formed through the reaction between degradation products (such as reactive sulphur, ammonia, and aniline species) with either SMX or other intermediates.

Most intermediates reached their maximum concentration for short treatment times (2-10 min), and by the end of the experiment (60 min) only 9 of them persist. Even for the persistent products the relative abundance started to decline before 60 min, implicitly showing that they can be successfully eliminated through prolonged treatment. Only one of these persistent products reaches a maximum abundance at 60 min.

The third experimental part of this thesis (**Chapter 5**) aimed to investigate the degradation of AMX and SMX in mono- and bi-component solutions (**O4**) using either a dielectric barrier discharge with falling liquid film or a corona discharge. The solution analysis allowed the identification of degradation intermediates (**O2**) and their monitoring during treatment (**O5**). For the dielectric barrier discharge reactor, the effect of the most important discharge parameters (applied voltage and average power) on antibiotic removal and energy efficiency, as well as the influence of the nature of the discharge gas (oxygen or air) were investigated.

In order to evaluate the effect of voltage on degradation, two voltage amplitudes were used: 13 and 15 kV, while adjusting the frequency to maintain an almost constant discharge power. Thus, the average power in the discharge was 12.2 W for 13 kV and 1 kHz and 12.9 W for 15 kV and 0.6 kHz. Pollutant removal has been well described by an exponential function, which corresponds to a pseudo-first order kinetic process. This allowed the calculation of an energy-dependent reaction rate constant (k_E). AMX degradation was slightly faster and more efficient when using a higher voltage amplitude. In the case of SMX, the concentration decreased in a similar manner to AMX, but the elimination did not seem to be influenced by the voltage amplitude over the investigated range.

Increasing the power dissipated in plasma (9.1-20.2 W) leads to faster degradation because higher concentrations of active species are formed, thus being available to react with organic molecules. However, taking into account the energy input, the degradation results are comparable regardless of the discharge power. A similar trend as a function of discharge power is observed for SMX, but with smaller differences, of only a few percent, over the investigated

power range. The energy yield for 50% degradation of the two pollutants was around 3.2-4 g/kWh for the dielectric barrier discharge configuration.

In order to evaluate the effect of the discharge gas, the plasma was generated either with oxygen or with air, using a voltage of 13 kV and a frequency of 600 Hz. The degradation of both antibiotics was significantly faster and more efficient in oxygen than in air: the half-life was about three times shorter, and k_E was 2.6 times higher. For the degradation of AMX and SMX in mixture, the initial concentration of each antibiotic was half the concentration used in the mono-component solutions. At first glance, both antibiotics appear to be degraded more rapidly in the binary solution as compared to the individual ones, with the difference being more noticeable for AMX than for SMX and for the air discharge than for O₂. The oxygen discharge produces comparable results in terms of degradation efficiency regardless of the solution composition (number of pollutants). SMX degradation using air as discharge gas was also similar for mono- and bi-component solutions. On the contrary, AMX removal in the air plasma was favoured in mixture, having a k_E (0.25 kJ⁻¹) considerably higher than the value obtained in the mono-component solution (0.15 kJ⁻¹). This behaviour could be attributed to the RNS contribution to the removal of this particular pollutant. A possible degradation pathway of AMX may consist of a hydrogen abstraction step through the attack of hydroxyl or sulfate radicals with formation of a phenoxy radical, followed by its rapid reaction with •NO₂. A contribution from species resulting from SMX degradation is also possible.

The degradation of AMX (100 mg/L) and SMX (80 mg/L) in mono- and bi-component solutions containing the same concentrations of pollutants has also been evaluated in the plasma-ozonation system operated with the optimized parameters. For SMX, k_E decreased three times in binary mixture compared to the mono-component solution, while for AMX, k_E only suffered a 25% reduction. Even though the decrease of k_E was expected due to the higher organic load in the solution, the different variations suggests that in mixture AMX is preferentially eliminated.

In order to better understand the degradation of the two antibiotics in the mixture, the previously identified intermediates for each of the contaminants were monitored. The use of another chromatographic method allowed the detection of four degradation intermediates of SMX with retention times longer than the target pollutant, compounds that were not addressed in the dedicated chapter. These compounds describe three additional degradation pathways

involving the oxidation of the amino group to nitro or coupling reactions of SMX with its degradation products.

The relative abundance of the degradation intermediates of AMX and SMX was evaluated in mono and bi-component solutions. The peak height of the extracted ion chromatograms for each of the intermediates were used to determine their relative abundance. For easy comparison of the two data sets, the values were normalized to the maximum recorded value, regardless of the set. For both pollutants, most of the identified degradation intermediates reached maximum abundance in the mono-component solution, and only a few form more abundantly when treated in mixture. The only explanation for this behaviour is that the target pollutants and their degradation intermediates influence each other directly or indirectly. In binary solution, in the case of AMX, sulphur oxidation reactions with the formation of sulfonated compounds, hydrolysis of the β -lactam cycle and decarboxylation are favoured. For SMX, the preferred reactions in mixture were hydroxylation and opening of the benzene ring, suggesting that the prevailing mechanisms are those based on hydroxyl radicals and ozone. For both pollutants investigated, the sulfonated intermediates had higher abundances in mixture compared to the mono-component solutions, thus showing an increased prevalence of the reactions with RSS.

When comparing the chromatograms obtained for the mono- and bi-component solutions (**Figure 5.**) a new peak was observed only for the mixture, which cannot be associated with any intermediate already identified. It was assigned to a degradation product formed through the association of the target pollutants noted as AS427.

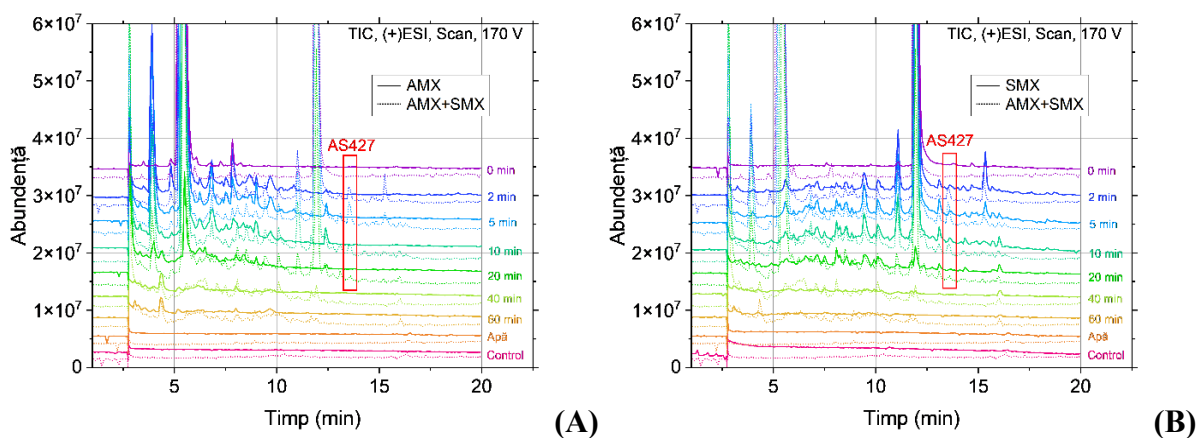


Figure 5. Total ion current (TIC) chromatograms representative for plasma degradation of AMX (A) and SMX (B) in mono- and bi-component solutions, for (+)ESI.

Starting from the fragmentation profiles of the two pollutants and the spectrum recorded for AS427, the structure of this intermediate was proposed, containing elements specific to the structure of both AMX and SMX. Thus, a reaction mechanism was proposed (**Figure 6.**) to explain the formation of this product from degradation intermediates already present in the solution at the beginning of the treatment process.

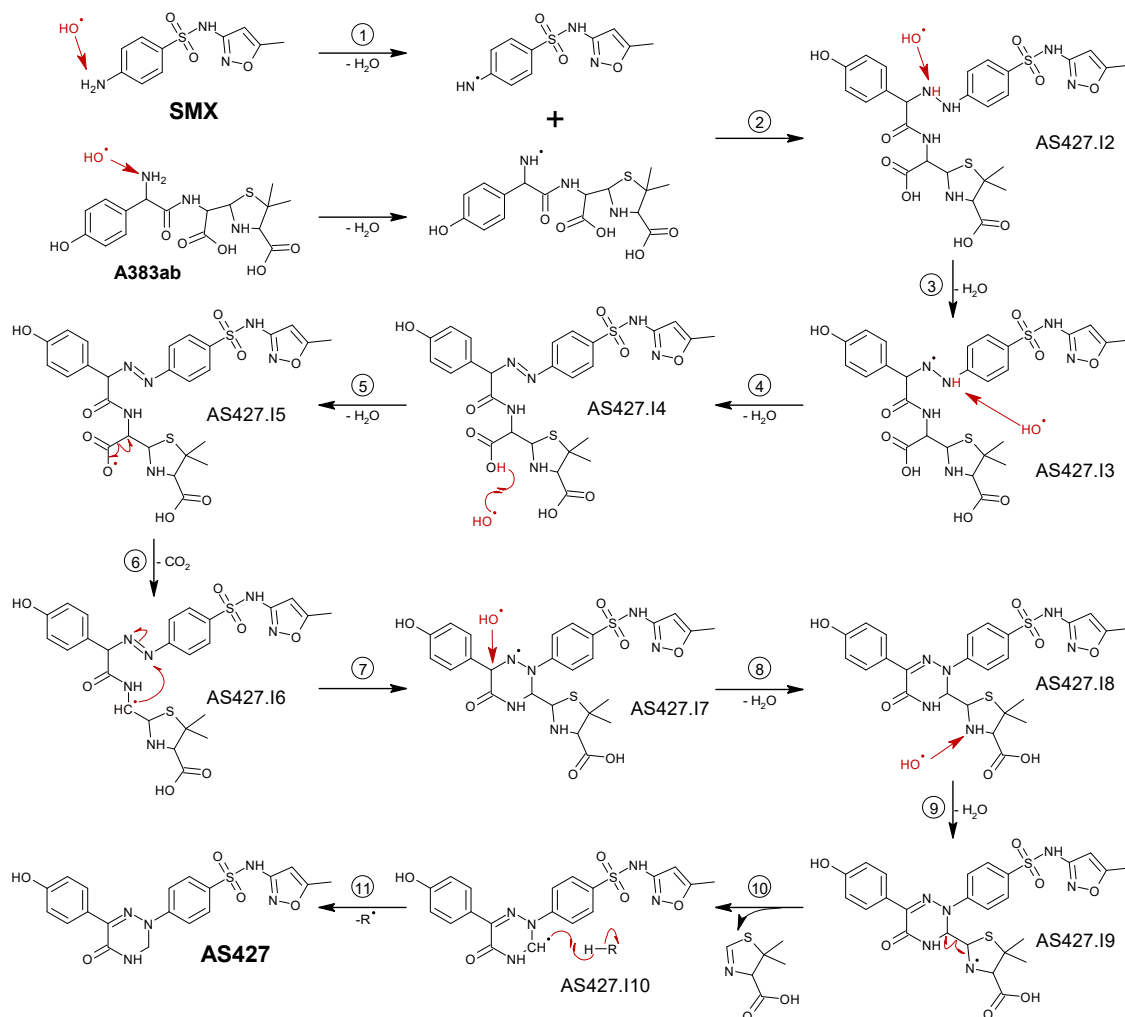


Figure 6. Proposed reaction mechanism for the formation of AS427 with the participation of reactive species generated in plasma.

SMX and penicilloic acids formed during AMX degradation serve as precursors. The first step of the proposed mechanism is hydrogen atom abstraction [28, 29], which leads to the formation of corresponding organic radicals that recombine yielding a hydrazine which is then oxidized to an azo group. This process is followed by radical decarboxylation which ends with

the formation of the triazine cycle. The last step involves cleavage of the C–C bond that connects the thiazolidine cycle to the rest of the molecule as a result of a radical fragmentation process. Along the way, the resulting organic radicals are stabilized by hydrogen atom abstraction from other compounds in the solution. Thus, in the case of the bi-component solution, multiple combination reactions (sulfonation and AS427 formation) have been highlighted, which are favoured by the water impurity matrix.

The fourth experimental part of this thesis (**Chapter 6**) focused on the effect of the water impurity matrix on the degradation of pollutants (AMX, DCD and IBU) by using mono-, bi- and multi-component solutions equated based on the theoretical oxygen demand (ThOD) (**O4**). In addition, the degradation intermediates of DCF and IBU (**O2**) and their formation mechanisms (**O3**) were identified and their abundance was monitored when changing the impurity matrix of the solution.

The difficulty encountered when comparing solutions with complex impurity matrices made necessary the use of an equivalence strategy for solutions with different concentrations of pollutants. Given that plasma degradation of organic compounds is mainly achieved via reactive oxygen species, an appropriate approach is to use ThOD as an equivalence parameter. In order to study the influence of the impurity matrix, the solutions were prepared in such a way that, regardless of the number and type of pollutants, the ThOD was the same. This strategy allowed the direct comparison of degradation in solutions of different complexity containing AMX, IBU and/or DCF as target pollutants.

To begin with, the degradation of AMX and IBU in mono- and multi-component solutions (together with DCF) with the same ThOD was compared. For both compounds, degradation is faster in mixture than in mono-component solutions. A possible explanation for these unexpected results is based on the reactions between the ions present in the solution and the ROS that lead to the formation of other oxidizing species. From the very beginning, sulfate ions are present in the solution. During treatment, as contaminant molecules degrade, Cl^- , NH_4^+ and NO_3^- are added to them. These ions can interact with plasma-generated species, leading to the formation of radical species with a more pronounced reaction specificity in relation to organic pollutants.

In order to obtain a more detailed perspective on the effect of the water impurity matrix on degradation, the number and quantity of pollutants in the solution were varied while maintaining the same ThOD. The degradation of IBU and DCF in mono-, bi- and multi-component solutions was compared. In this case the binary solutions were prepared with a target pollutant concentration of 0.1 mM, adjusting the ThOD by adding AMX. In general, among the solutions with the same ThOD, the fastest degradation was achieved in multi-component solutions, followed by bi-component solutions and finally mono-component ones.

The degradation of pollutants in multi-component solutions was evaluated with or without buffering the solution, by using for conductivity adjustment sodium bicarbonate and sodium sulfate, respectively. Solution buffering had a positive effect on AMX degradation, but did not significantly influence IBU elimination. DCF removal occurs more rapidly in sodium sulfate solution. DCF dechlorination takes place similarly for the two multi-component solutions (with the addition of NaHCO₃ or Na₂SO₄), reaching 99% after 60 min of treatment. The mineralization of nitrogen in the structure of pollutants reached 55.3% of the total theoretical amount, the main species formed being NO₃⁻ and NH₄⁺. The mineralization of sulfur (in the form of sulfate ions) reached a maximum of 60%.

The identification of degradation products in mono-component solutions was performed for IBU and DCF by employing the same chromatographic method used for the identification of AMX intermediates. The MS² spectra recorded in both (+)ESI and (-)ESI were used. In the case of IBU, in (-)ESI, the main mass transition is (-)m/z 205 → (-)m/z 161 ($\Delta m = 44$ u) which describes the loss of the carboxyl group as CO₂ [27], the others representing minor transitions, poorly represented in the mass spectrum. In (+)ESI, the [M+H]⁺ pseudomolecular ion associated with IBU was not identified. Instead, the ion [M-HCOO]⁻ was recorded with (+)m/z 161.

Based on the mass spectra recorded, 33 degradation intermediates were identified, three of which were also reported in other plasma degradation studies of IBU [30–32]. Of these products, four were identified based on mass spectra available in the Massbank database [33]. The identified intermediates were grouped into four main degradation pathways. The first of these involves the hydroxylation of the tertiary carbon of the isobutyl group for which a two step reaction mechanism has been proposed. This mechanism involves hydrogen atom abstraction and the combination of the resulting organic radical with a hydroxyl radical. The hydroxylation through the addition to a double bond of benzene describes the start of another degradation

pathway. The other two degradation pathways identified involved oxidation of the methyl group to carbonyl and decarboxylation of IBU. During the degradation of the intermediates, the main reactions that took place were opening the benzene ring, oxidation, decarboxylation and fragmentation. The mechanism of benzene ring cleavage through the reaction with ozone was the one presented above (**Figure 2.**). In the case of decarboxylation, three mechanisms have been proposed (**Figure 7.**). The first two involve hydrogen atom abstraction following the attack of HO^\bullet with the formation of water and an organic radical. The latter spontaneously releases CO_2 , and the resulting radical either combines with a hydroxyl radical to form an alcohol or participates in another hydrogen atom abstraction. The third decarboxylation mechanism involves the formation of an organic radical with an unpaired electron at the carbon atom adjacent to the carboxyl group, which attacks an oxygen molecule forming an unstable peroxide radical. This compound undergoes the intramolecular transfer of a hydrogen atom resulting in the removal of CO_2 and HO^\bullet and the formation of a ketone [34]. Most IBU intermediates reach maximum abundance at short treatment times (5-20 min), but some persist even after 60 min.

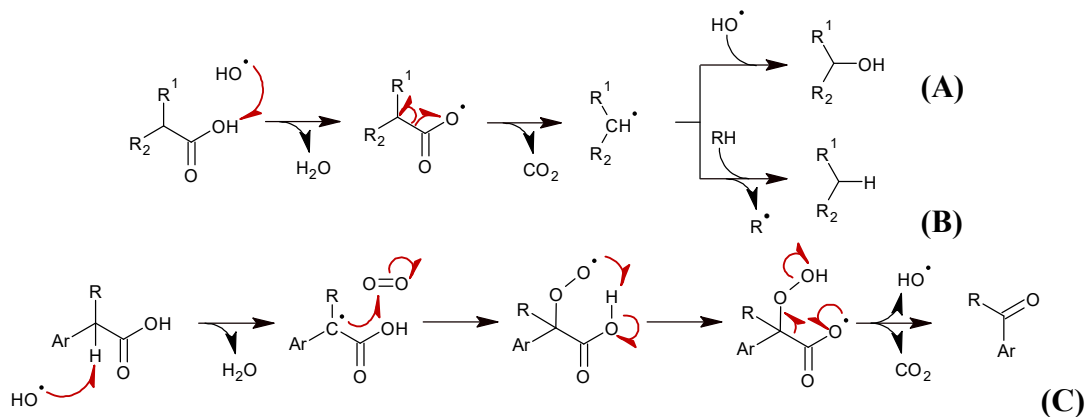


Figure 7. The proposed mechanisms for decarboxylation with **(A)** and without **(B)** hydroxylation or **(C)** the formation of ketones.

When identifying the degradation products of DCF, the isotopic profile plays an important role because the number of chlorine atoms in the structure leads to a specific isotopic profile. Thus, the m/z , $m/z+2$ and $m/z+4$ ions in the isotopic profile of the pseudomolecular ion will have an abundance ratio of 9:6:1 for all compounds containing two chlorine atoms, as a result of the natural abundance of chlorine isotopes. In total, 23 degradation intermediates of DCF have been identified, of which 12 have already been reported in other plasma degradation

studies concerning this pollutant [35–39]. A special case when identifying the degradation intermediates of DCF is D588. This time a specific isotopic profile observed correlates with the presence of four chlorine atoms in the structure of the compound. As a result, the monoisotopic pseudomolecular ion ends up not having the maximum abundance in the group of ions that describe the isotopic profile. Together with the MS² spectra recorded, D588 has been identified as a dimer of DCF.

The degradation intermediates were grouped into five distinct degradation pathways. One of these is dimerization with the formation of D588. Two other pathways describe the alternative hydroxylation of the two benzene rings of DCF, most likely though the mechanism of hydroxyl radical addition to the double bond. The last two degradation pathways start from the dechlorination of the pollutant. This reaction can take place through two mechanisms (**Figure 8**). The first of these involves the addition of HO• to the double bond at one of the chlorine-substituted carbon atoms with the formation of an organic radical that releases HCl. The resulting unstable intermediate participates in the abstraction of a hydrogen atom [40]. The second mechanism involves the reaction with hydrated electrons generated in the plasma that results in dechlorination and the formation of an organic radical which undergoes cyclization. All degradation intermediates of DCF register maximum abundance in the first 10 min of treatment and most become undetectable at longer treatment times (40-60 min).

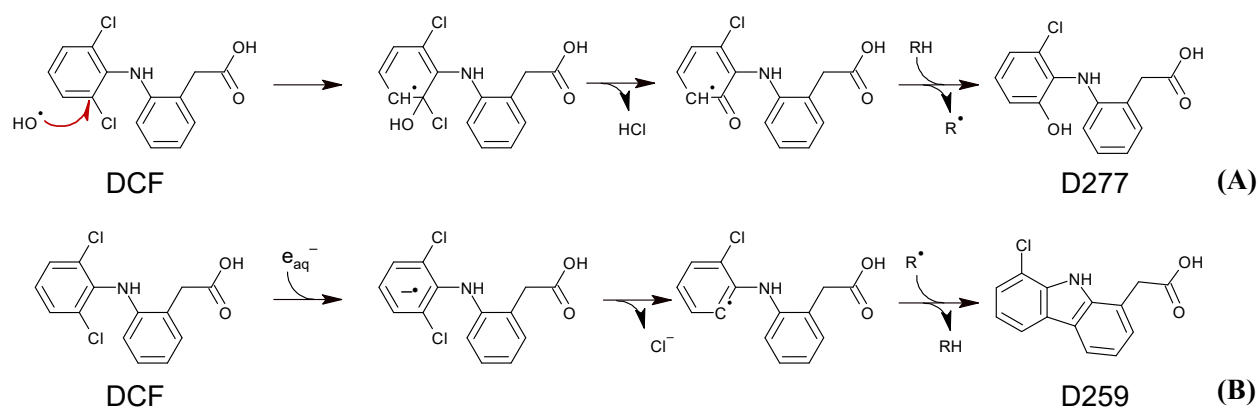


Figure 8. Proposed mechanisms for dechlorination of DCF by (A) HO• or (B) e_{aq}⁻ attack.

The analysis of degradation intermediates through the same chromatographic method allowed the comparison of the results obtained for mono- and multi-component solutions. All the peaks recorded in the chromatograms associated with the multi-component solution were

correlated with peaks of the different degradation products recorded for one of the three pollutants tested (AMX, DCF, IBU). This correlation was made based on the retention time, but also on the MS and MS² mass spectra recorded. Thus, unlike the case of the AMX-SMX binary solution, where SMX is combined with AMX degradation products, resulting in the AS427 intermediate, the impurity matrix of multi-component samples does not favour the combination reactions between intermediates from different target pollutants with the formation of specific degradation products. This does not, however, exclude other types of cross-reactions that may occur, which would explain the superior degradation of target pollutants in solutions with complex impurity matrices. Such reactions include the hydrogen atom abstraction through the reaction with organic radicals (from the degradation of pollutants) or inorganic radicals (such as hydroxyl radicals) and reactions with reactive chlorine, nitrogen or sulfur species resulted from the degradation products of the tested contaminants.

The results presented in the four experimental chapters prove the fulfilment of all the objectives proposed in this thesis. I have selected the most suitable configuration of the plasma treatment system, as well as the optimal parameters for its operation so that the degradation of pollutants is achieved quickly and efficiently. I have identified the intermediates obtained during the plasma degradation of all pollutants investigated, both in single-component solutions and in mixtures. I have identified and proposed multiple mechanisms involved in the degradation of pollutants tested in solutions with complex impurity matrix, including combination mechanisms that lead to the formation of degradation intermediates specific to mixtures. I have successfully evaluated the variation of the abundance of degradation intermediates, of their structure and of the reaction mechanisms that take place when changing the impurity matrix.

Thus, the main direct effect of the water impurity matrix on degradation is given by the generation of reactive species originating from pollutant degradation that subsequently assist their removal and the elimination of their intermediates, be it reactive species of chlorine, nitrogen, sulfur or even organic radical species. Among the mechanisms identified regardless of solution complexity, the most prevalent were the two-step hydroxylation mechanism by addition to the double bond and the benzene ring opening through the reaction with ozone.

Selective bibliography:

- [1] Ritter K., Solomon P., Sibley L., 2002. Sources, pathways, and relative risks of contaminants in surface water and groundwater: a perspective prepared for the walkerton inquiry. *J. Toxicol. Environ. Health A* 65, 1–142. <https://doi.org/10.1080/152873902753338572>
- [2] The European Parliament and the Council of the European Union, 2000. Directive 2000/60/EC of the European Parliament and the Council of 23 October 2000 establishing a framework for Community action in the field of water policy. *OJEC* 327, 35–38
- [3] Harrison R.M., 2007. *Understanding our Environment: An Introduction to Environmental Chemistry and Pollution*. Ed. Harrison RM. Royal Society of Chemistry, Cambridge. <https://doi.org/10.1039/9781847552235>
- [4] EC, 1983. Protocol for the Protection of the Mediterranean Sea against Pollution from Land-based Sources. *OJEC*. <https://doi.org/10.1163/221160082x00305>
- [5] The European Parliament and the Council of the European Union, 2008. Directive 2008/105/EC of the European Parliament and of the Council of 16 December 2008 on environmental quality standards in the field of water policy, amending and subsequently repealing Council Directives 82/176/EEC, 83/513/EEC, 84/156/EEC, 84/491/EEC, 86/280/EEC and amending Directive 2000/60/EC of the European Parliament and of the Council. *OJEU* L348, 84–97.
- [6] European Commission, 2015. Commission Implementing Decision (EU) 2015/495 of 20 March 2015 establishing a watch list of substances for Union-wide monitoring in the field of water policy pursuant to Directive 2008/105/EC of the European Parliament and of the Council. *OJEU* L78/40, 20–30.
- [7] The European Commission, 2018. Commission Implementing Decision (EU) 2018/ 840 - of 5 June 2018 - establishing a watch list of substances for Union-wide monitoring in the field of water policy pursuant to Directive 2008/ 105/ EC of the European Parliament and of the Council and repealing Commission Implementing Decision (EU) 2015/ 495 - (notified under document C(2018) 3362). *OJEU* L141, 9–12.
- [8] The European Commission, 2020. Commission Implementing Decision (EU) 2020/1161 of 4 August 2020 establishing a watch list of substances for Union-wide monitoring in the

field of water policy pursuant to Directive 2008/105/EC of the European Parliament and of the Council. OJEU L257, 32–35.

- [9] The European Commission, 2022. Commission Implementing Decision (EU) 2022/1307 of 22 July 2022 establishing a watch list of substances for Union-wide monitoring in the field of water policy pursuant to Directive 2008/105/EC of the European Parliament and of the Council. OJEU L 197,117–120.
- [10] The European Commission, 2025. Commission Implementing Decision (EU) 2025/439 of 28 February 2025 establishing a watch list of substances for Union-wide monitoring in the field of water policy pursuant to Directive 2008/105/EC of the European Parliament and of the Council. OJEU L2025/439.
- [11] Verlicchi P., Galletti A., Petrovic M., Barceló D., 2010. Hospital effluents as a source of emerging pollutants: An overview of micropollutants and sustainable treatment options. *J. Hydrol. (Amst)* 389, 416–428. <https://doi.org/10.1016/j.jhydrol.2010.06.005>
- [12] Madikizela L.M., Ncube S., Chimuka L., 2020. Analysis, occurrence and removal of pharmaceuticals in African water resources: A current status. *J. Environ. Manage.* 253, 109741. <https://doi.org/10.1016/j.jenvman.2019.109741>
- [13] Silori R., Shrivastava V., Singh A., Sharma P., Aouad M., Mahlknecht J., Kumar M., 2022. Global groundwater vulnerability for Pharmaceutical and Personal care products (PPCPs): The scenario of second decade of 21st century. *J. Environ. Manage.* 320, 115703. <https://doi.org/10.1016/j.jenvman.2022.115703>
- [14] Bijlsma L., Pitarch E., Fonseca E., Ibáñez M., Botero A.M., Claros J., Pastor L., Hernández F., 2021. Investigation of pharmaceuticals in a conventional wastewater treatment plant: Removal efficiency, seasonal variation and impact of a nearby hospital. *J. Environ. Chem. Eng.* 9, 105548. <https://doi.org/10.1016/j.jece.2021.105548>
- [15] Serna-Galvis E.A., Botero-Coy A.M., Rosero-Moreano M., Lee J., Hernández F., Torres-Palma R.A., 2022. An Initial Approach to the Presence of Pharmaceuticals in Wastewater from Hospitals in Colombia and Their Environmental Risk. *Water (Basel)* 14, 950. <https://doi.org/10.3390/w14060950>
- [16] Moratalla Á., Cotillas S., Lacasa E., Fernández-Marchante C.M., Ruiz S., Valladolid A., Cañizares P., Rodrigo M.A., Sáez C., 2022. Occurrence and toxicity impact of

- pharmaceuticals in hospital effluents: Simulation based on a case of study. *Process Saf. Environ. Prot.* 168, 10–21. <https://doi.org/10.1016/j.psep.2022.09.066>
- [17] Arvaniti O.S., Arvaniti E.S., Gyparakis S., Sabathianakis I., Karagiannis E., Pettas E., Gkotsis G., Nika M.C., Thomaidis N.S., Manios T., Fountoulakis M.S., Stasinakis A.S., 2023. Occurrence of pharmaceuticals in the wastewater of a Greek hospital: Combining consumption data collection and LC-QTOF-MS analysis. *Sci. Total Environ.* 858. <https://doi.org/10.1016/j.scitotenv.2022.160153>
- [18] Paíga P., Correia M., Fernandes M.J., Silva A., Carvalho M., Vieira J., Jorge S., Silva J.G., Freire C., Delerue-Matos C., 2019. Assessment of 83 pharmaceuticals in WWTP influent and effluent samples by UHPLC-MS/MS: Hourly variation. *Sci. Total Environ.* 648, 582–600. <https://doi.org/10.1016/j.scitotenv.2018.08.129>
- [19] Kosma C.I., Kapsi M.G., Konstas P.S.G., Trantopoulos E.P., Boti V.I., Konstantinou I.K., Albanis T.A., 2020. Assessment of multiclass pharmaceutical active compounds (PhACs) in hospital WWTP influent and effluent samples by UHPLC-Orbitrap MS: Temporal variation, removals and environmental risk assessment. *Environ. Res.* 191. <https://doi.org/10.1016/j.envres.2020.110152>
- [20] de Oliveira M., Frihling B.E.F., Velasques J., Filho F.J.C.M., Cavalheri P.S., Migliolo L., 2020. Pharmaceuticals residues and xenobiotics contaminants: Occurrence, analytical techniques and sustainable alternatives for wastewater treatment. *Sci. Total Environ.* 705, 135568. <https://doi.org/10.1016/j.scitotenv.2019.135568>
- [21] The European Parliament and the Council of the European Union, 2024. Directive (EU) 2024/3019 of the European Parliament and of the Council of 27 November 2024 concerning urban wastewater treatment (recast). OJEU L2024/3019.
- [22] Miklos D.B., Remy C., Jekel M., Linden K.G., Drewes J.E., Hübner U., 2018. Evaluation of advanced oxidation processes for water and wastewater treatment – A critical review. *Water Res.* 139, 118–131. <https://doi.org/10.1016/j.watres.2018.03.042>
- [23] Bruggeman P.J., Kushner M.J., Locke B.R., Gardeniers J.G.E., Graham W.G., Graves D.B., Hofman-Caris R.C.H.M., Maric D., Reid J.P., Ceriani E., Fernandez Rivas D., Foster J.E., Garrick S.C., Gorbanev Y., Hamaguchi S., Iza F., Jablonowski H., Klimova E., Kolb J., Krema F., Lukes P., MacHala Z., Marinov I., Mariotti D., Mededovic Thagard S., Minakata D., Neyts E.C., Pawlat J., Petrovic Z.L., Pflieger R., Reuter S., Schram D.C.,

- Schröter S., Shiraiwa M., Tarabová B., Tsai P.A., Verlet J.R.R., Von Woedtke T., Wilson K.R., Yasui K., Zvereva G., 2016. Plasma-liquid interactions: A review and roadmap. *Plasma Sources Sci. Technol.* 25. <https://doi.org/10.1088/0963-0252/25/5/053002>
- [24] Locke B.R., Sato M., Sunka P., Hoffmann M.R., Chang JS, 2006. Electrohydraulic discharge and nonthermal plasma for water treatment. *Ind. Eng. Chem. Res.* 45:882–905. <https://doi.org/10.1021/ie050981u>.
- [25] Lukes P., Clupek M., Babicky V., Janda V., Sunka P., 2005. Generation of ozone by pulsed corona discharge over water surface in hybrid gas-liquid electrical discharge reactor. *J. Phys. D Appl. Phys.* 38, 409–416. <https://doi.org/10.1088/0022-3727/38/3/010>
- [26] Lukes P., Appleton A.T., Locke B.R., 2004. Hydrogen Peroxide and Ozone Formation in Hybrid Gas-Liquid Electrical Discharge Reactors. *IEEE Trans. Ind. Appl.* 40, 60–67. <https://doi.org/10.1109/TIA.2003.821799>
- [27] Holčapek M., Jirásko R., Lísa M., 2010. Basic rules for the interpretation of atmospheric pressure ionization mass spectra of small molecules. *J. Chromatogr. A* 1217, 3908–3921. <https://doi.org/10.1016/j.chroma.2010.02.049>
- [28] Allais C., Hansen E.C., Ide N.D., Perkins R.J., Swift EC, 2020. Selected Free Radical Reactions. In: *Practical Synthetic Organic Chemistry*. Wiley, pp 563–589. <https://doi.org/10.1002/9781119448914.ch11>.
- [29] Renaud P., Sibi M.P., 2001. *Radicals in Organic Synthesis*, 1st edition. WILEY-VCH Verlag GmbH, Weinheim
- [30] Sohrabi A., Haghghat G., Shaibani P.M., Van Neste C.W., Naicker S., Sadrzadeh M., Thundat T., 2019. Degradation of pharmaceutical contaminants in water by an advanced plasma treatment. *Desalination Water Treat.* 139, 202–221. <https://doi.org/10.5004/dwt.2019.23297>
- [31] Li Z., Wang Y., Guo H., Pan S., Puyang C., Su Y., Qiao W., Han J., 2021. Insights into water film DBD plasma driven by pulse power for ibuprofen elimination in water: performance, mechanism and degradation route. *Sep. Purif. Technol.* 277, 119415. <https://doi.org/10.1016/j.seppur.2021.119415>
- [32] Marković M., Jović M., Stanković D., Kovačević V., Roglić G., Gojgić-Cvijović G., Manojlović D., 2015. Application of non-thermal plasma reactor and Fenton reaction for

- degradation of ibuprofen. *Sci. Total Environ.* 505, 1148–1155. <https://doi.org/10.1016/j.scitotenv.2014.11.017>
- [33] Horai H., Arita M., Kanaya S., Nihei Y., Ikeda T., Suwa K., Ojima Y., Tanaka K., Tanaka S., Aoshima K., Oda Y., Kakazu Y., Kusano M., Tohge T., Matsuda F., Sawada Y., Hirai M.Y., Nakanishi H., Ikeda K., Akimoto N., Maoka T., Takahashi H., Ara T., Sakurai N., Suzuki H., Shibata D., Neumann S., Iida T., Tanaka K., Funatsu K., Matsuura F., Soga T., Taguchi R., Saito K., Nishioka T., 2010. MassBank: a public repository for sharing mass spectral data for life sciences. *J. Mass Spectrom.* 45, 703–714. <https://doi.org/10.1002/jms.1777>
- [34] Gangadurai C., Illa G.T., Reddy D.S., 2020. FeCl₃-catalyzed oxidative decarboxylation of aryl/heteroaryl acetic acids: Preparation of selected API impurities. *Org. Biomol. Chem.* 18, 8459–8466. <https://doi.org/10.1039/d0ob01790f>
- [35] Banaschik R., Jablonowski H., Bednarski P.J., Kolb J.F., 2018. Degradation and intermediates of diclofenac as instructive example for decomposition of recalcitrant pharmaceuticals by hydroxyl radicals generated with pulsed corona plasma in water. *J. Hazard. Mater.* 342, 651–660. <https://doi.org/10.1016/j.jhazmat.2017.08.058>
- [36] Kumar A., Škoro N., Gernjak W., Jovanović O., Petrović A., Živković S., Lumbaue E.C., Farré M.J., Puač N., 2023. Degradation of diclofenac and 4-chlorobenzoic acid in aqueous solution by cold atmospheric plasma source. *Sci. Total Environ.* 864, 161194. <https://doi.org/10.1016/j.scitotenv.2022.161194>
- [37] Nippatlapalli N., Ramakrishnan K., Philip L., 2022. Enhanced degradation of complex organic compounds in wastewater using different novel continuous flow non – Thermal pulsed corona plasma discharge reactors. *Environ. Res.* 203, 111807. <https://doi.org/10.1016/j.envres.2021.111807>
- [38] Singh R.K., Philip L., Ramanujam S., 2017. Rapid degradation, mineralization and detoxification of pharmaceutically active compounds in aqueous solution during pulsed corona discharge treatment. *Water Res.* 121, 20–36. <https://doi.org/10.1016/j.watres.2017.05.006>
- [39] Liu Q., Ouyang W., Yang X., He Y., Wu Z., Ostrikov K. (Ken), 2023. Plasma-microbubble treatment and sustainable agriculture application of diclofenac-contaminated wastewater. *Chemosphere* 334, 138998. <https://doi.org/10.1016/j.chemosphere.2023.138998>

- [40] He Y., Wu J., Fang X., von Sonntag C., 1997. Hydroxyl-radical induced dechlorination of pentachlorophenol in water. In: Radiation technology for conservation of the environment. Proceedings of a symposium. pp 273–280.